Numerical Simulation of Infrared Staking Plastic for an Automotive Part

†*Hong- Seok Park[1], Trung-Thanh Nguyen[1]

[1]School of Mechanical Engineering, University of Ulsan, 93 Daehak-ro, Nam-gu, Ulsan, South-Korea, 680-749

*Presenting author: phosk@ulsan.ac.kr
†Corresponding author: phosk@ulsan.ac.kr

Abstract

Staking plastic is a new technology that used infrared light as the energy sources in order to assembly the heated plastic parts. In this work, the proposed method coupling between Finite Element Method (FEM), Response Surface Method, and Genetic Algorithm (GA) is employed to simulate and optimize the staking plastic process. An automotive part, namely Door Trim with polypropylene (PP) material is implemented by using the developed technology. The effects of three key process parameters, such as heating time, cooling time, and air flow rate on the mechanical behavior of the joint has been investigated. The simulation procedure based on DEFORM-3D Multi-operation is conducted to integrate sub-process and obtain the numerical results. The optimum values, including heating time, cooling time, and air flow rate are 14 second, 14 second, and 60 (ft^3/h), respectively. The optimizing results indicated that heating time is more contributed to the tensile force, following by cooling time and air flow rate. The correlation between simulation and experimental results indicates the effectiveness of the proposed method.

Keywords: Staking plastic, Door Trim, DEFORM-3D-based Multi-operation, Tensile strength, Genetic algorithm

Introduction

The infrared staking process was developed by EXTOL by using halogen lighting in order to procedure the joint between different plastic part [Extolinc]. In comparison with the conventional staking technology using heat, hot air, and ultrasonic source, this process provides some advantages, such as higher energy efficiency, product quality, productivity, and better mechanical properties. The process takes place in four basic phases that can be listed as follows (Fig.1):

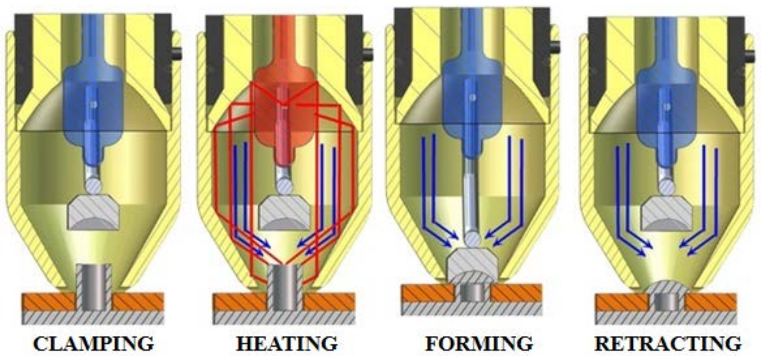

Fig.1 Infrared staking process [Extolinc]

Clamping: The infrared staking module is positioned over the molded stud or boss to ensure perfect contact with the plastic part. The concentrator directly makes contact with the upper part, clamping it to the lower part and holding them in the proper position. As an added benefit, due to the ideal clamping at the stake points, secondary part clamps are not necessary.

Heating: The energy source used in the infrared staking process is a 12-Volt, 100-Watt, technical-grade of a halogen lamp. The reflector directly transfers the infrared energy from the lamp into a stud around the punch. This column of energy travels downward until it is focused on the full perimeter of the boss, heating it from top to bottom. To make this possible, the surface geometry of both the reflector and the concentrator creates a focal area that is centered on the boss. Ideally, the stud can be heated as quickly and as evenly as possible.

Staking & Cooling: At the end of the heating cycle, the lamp is switched off and the low-impact air cylinder with integrated staking punch is employed which forms over the semi-molten stud. The gold plating and the perfect contact area between the punch and formed part can reduce the temperature of the molten plastic quickly. The cooling air will be flowing into the chamber in order to assist in regulating the punch temperature which prevents the plastic from sticking to it.

Punch Retracts: At the end of the punch time, the punch retracts. The module is retracted from the components, and the cycle is completed. The sub-assembly can be immediately handled. At this point, it is important that the plastic has re-solidified to the point where it can maintain its shape and structure.

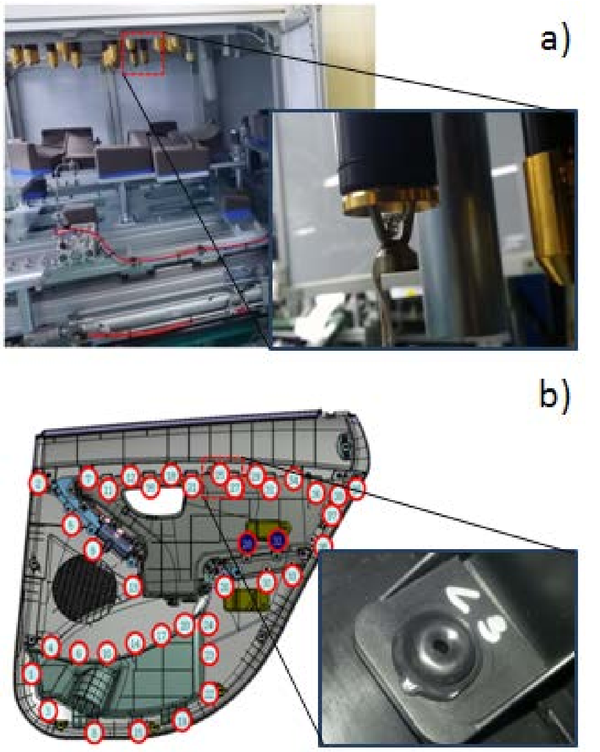

Fig.2 Machine and completed product; a-Developed machine and dies, b-assembled door trim and completed joint

In this project, we attempt to develop new machine, which used to assemble the different plastic components of Door Trim. The joint is generated based on PP material and an infrared staking process. The machine, dies, assembled Door Trim, and completed product are shown in Fig.2. Recently, this technology is still a lack of the publications. In addition, identification of optimal values and understanding the effects of process parameters on the mechanical behavior after process are necessary. To solve this problem, this paper proposed an approach to simulate and optimize whole staking process. The key sub-process, including heating, forming, and cooling is integrated into one simulation model. The developed finite element (FE) model considering the data history based on DEFORM-3D Multi operation [Fluhrer, J (2005)] was adopted to conduct the serial numerical experiments. The coupling RSM using Box-Behnken experimental designs [C.F. Jeff et al. (200)] and GA is used to obtain the optimal values. Finally, the numerical results are compared with physical experiment to validate the effectiveness of the proposed method.

The proposed approach

The effected parameters on the tensile strength are listed in Fig. 3. In this work, we only consider process parameters due to the fixed of forming tool, machine, and material properties.

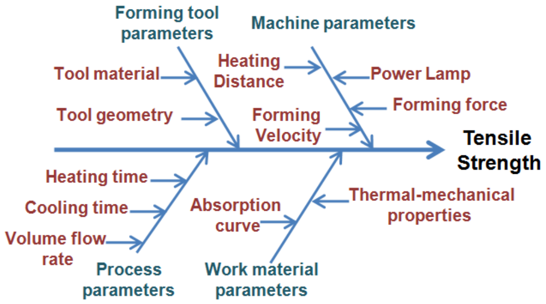

Fig.3 The effected parameters on the tensile strength

To investigate the material behavior, the sub-process has to integrate into one simulation model, in which the elements have the connection (Fig.4). In other words, the results of preceding process are inputs for the next step. The material state is changed by every step in the production process. The behavior of the final part will depend on the results of each step. After sub-process, the material properties and the stress, and the strain state have changed. Therefore the properties of the joints have to be included in a parameterized way. Transferring data between the simulation processes includes geometric, stress, and strain history [M. Oudjene et al. (2009)], [F. Lambiase et al. (2013)].

Multi-operation in DEFORM-3D was employed to simulate process chains. In the first stage, the simulation model is developed with material model, friction, and heat transfer conditions. After that, the forming process is conducted using boundary conditions. Consequently, these results are transferred to a cooling process considering two kinds of heat transfer, including conduction and convection. Finally, the tensile testing is conducted with the results of the previous stage.

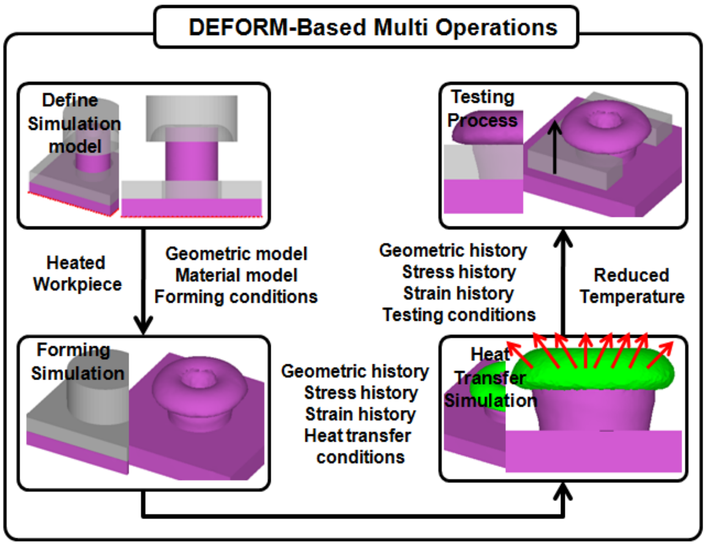

Fig.4 The approach for simulations of the whole process

Governing equations of forming simulation

Material model

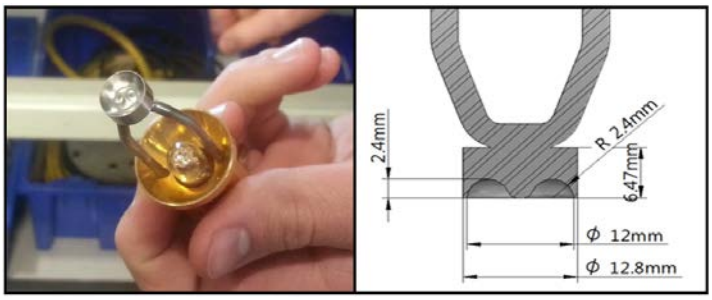

Fig.5 Geometric dimensions of die

A material model includes physical and thermal properties of the work piece and tool. Due to the fact that metal cutting and forming operations perform in high temperature and high strain rates, mechanical properties of work piece material are exactly known. Material properties of plastic-PP and die-S45C are shown in Table 1

Table 1 Material property of PP and S45C [Matweb]

Parameters	PP	S45C
Density (g/mm^3)	0.892 x10^{-3}	7.85 x10^{-3}
Young modulus (MPa)	1300	250x10^3
Poison ratio	0.45	0.29
Thermal conductivity(W/mm °C)	0.16x10^{-3}	49.8
Specific heat (J/g °C)	2	0.486

To save the simulation time and increase the accuracy, the tooling was modeled as perfectly rigid, while the work piece was considered as Elasto-plastic properties with isotropic hardening law and following Vonmises Stress yield criterion. FE model of die and PP work piece are consist of tetrahedral elements with four nodes. Flow stress curves of work piece materials must be used especially in the forming analysis. Flow stress curves of PP material change as a function strain, strain rate, and temperature is shown in Fig.6 at the strain 5min-1, 0.5min-1, and 0.05min-1. This law was selected due to its ability to follow the true behavior of a material [YUANXIN ZHOU et al (2002)]:

$$\bar{\sigma} = (\bar{\varepsilon}, \dot{\bar{\varepsilon}}, T) \qquad (1)$$

According to above Eq, σ is flow stress, ε and $\dot{\varepsilon}$, and T are effective plastic strain, effective strain rate, and temperature, respectively.

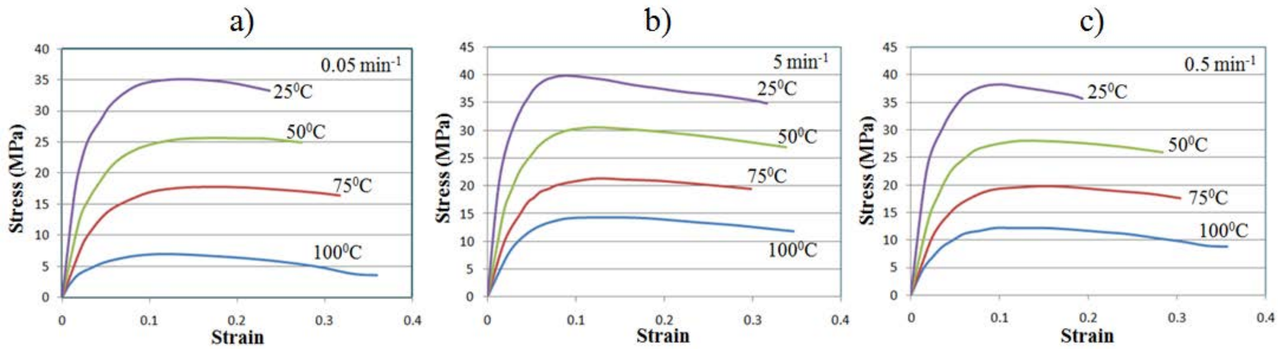

Fig.6 Stress-strain curves of polypropylene; (a) at the 0.05 min-1, (b)at the 5 min-1; (c) at the 0.5 min-1

Friction model

The friction types allowed are shear and coulomb friction. Shear (sticking); constant shear friction is used mostly for bulk-forming simulations. The frictional force in the constant shear model is defined by:

$$f_s = mk \qquad (2)$$

Where f_s is the frictional stress, k is the shear yield stress and m is the friction factor. Coulomb friction is used when contact occurs between two elastically deforming objects (could include an elastic-plastic object, if it is deforming elastically) or an elastic object and a rigid object, generally to model sheet-forming processes. The frictional force in the Coulomb law model is defined by:

$$f_s = \mu p \qquad (3)$$

Where f_s is the frictional stress, p is the interface pressure between two bodies and μ is the friction factor. There must be interfacial pressure between two bodies for frictional force to be present. Due to the complexity of the process, the hybrid friction model was used together both of Coulomb and shear friction models. To obtain the best simulation results, the preliminary simulations were carried out and μ =0. 3 was selected.

Heat transfer

The initial temperature of the ambient was assumed as 20 °C. The plastic temperature reaches 29 °C (after 8 second), 38 °C (after 14 second) and 43 °C (after 20 second), respectively. The heat losses to the environment from the free surface of the work piece material are determined by the heat flux:

$$Q = h(T - T_0) \qquad (4)$$

Where h = 4.5 W/m^{2}K is the heat transfer coefficient of the work material. T and T_0 are the temperature of the work material and ambient temperature, respectively.

Governing equations of heat transfer simulation

Two kinds of heat transfer are parallel conducted: convection and radiation. The plastic temperature is reduced due to conductive heat exchange with the die that decreases the temperature by forced convective heat transfer (Fig.7). According to the heat transfer theory and thermal equilibrium relationship by referring to the Fourer Role, the governing equation is established and given as follows:

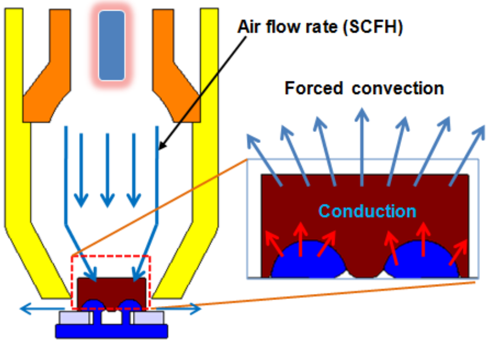

Fig.7 Heat transfer in the cooling process

$$k\left(\frac{\partial^2 T}{\partial x^2}+\frac{\partial^2 T}{\partial y^2}+\frac{\partial^2 T}{\partial z^2}\right)=\rho C\frac{\partial T}{\partial t}+Q \qquad (5)$$

Where k is the thermal conductivity, ρ is density, C is the specific heat, Q is the latent heat of phase transformation, x, y, z are the coordinates, and it is the time respectively. For the thermal boundary conditions, the adiabatic condition was employed for the others. The heat flow by conduction between the polymer and die [Carlaw, H et al (1959)] can be described as bellow:

$$\dot{Q}=-\frac{kA(\theta_f-\theta_0)}{\sqrt{\pi\alpha t}} \qquad (6)$$

Where, θ_0 is considered at the initial time and the final temperature after cooling is assumed to be at θ_f, α is the thermal diffusivity of the polymer, A denotes the cross sectional area, and t is the cooling time, respectively.

Optimization process

Response surface methodology (RSM) is adopted to establish a relationship between process parameters and the performance of objective functions. RSM is a well-known method with higher accuracy and better ease-of use than other popular meta-models, such as radial basis function and kriging model. The second-order RSM model is suitable for modeling the moderate non-linear behavior with few design variables. Prior to the optimization process, relationships between process parameters and objective functions should be created. In this research, the experimental plans are generated using the stipulated conditions using the Box-Behnken experimental designs with 17 runs. Box-Behnken experimental method is one of the effective designs based on multi-dimensional sphere and all the design points lie on a same sphere with at least three or six runs at the center point. The optimization process was resolved based on explicit equations in regression that were obtained through the previous approximation.

The process parameters, including heating time, cooling time, and air flow rate with three levels are listed in Table 2. The sequential simulations are conducted by using boundary conditions to obtain the simulation results that can be used to generate the mathematic model of tensile force (Eq.7).

Table 2 The level of parameters

Code	Parameters	Value
A	Heating time (s)	8-14-20
B	Cooling time (s)	8-14-20
C	Air flow rate (ft^3/h)	20-40-60

$$F=630.38+47.65*A+63.32*B+5.53*C+0.2286*A*B-0.0536*B*C-1.6*A^2-2.2*B^2-0.041*C^2 \quad (7)$$

Fig.8 shows the response surfaces, which show the effect of three key process parameters at the center point in the design space of the tensile force. It can be easily seen from the picture that heating time and cooling time have a large effect on the tensile strength, while volume air flow rate has a little effect on the objective function. The main reasons can be explained as follows. Too low heating time results in poor heat transfer and poor mixing material, thus causing of weak joint. Increasing the heating time increases the heat input to the material, resulting in better fusion, consequently, joint strength increases. However, a further heating time combining with forming pressure decreases the joint strength due to material decomposed and a weak joint is formed. Increasing the cooling time results in reducing more temperature that increases the joint strength. The input energy can be loss due to the diffusion at the contact area. Thus, higher cooling time may lead to decrease the tensile strength. Air flow rate has a significant effect to the tensile force. Increasing the air flow rate leads to reduce temperature and to improve the rigidity of workpiece.

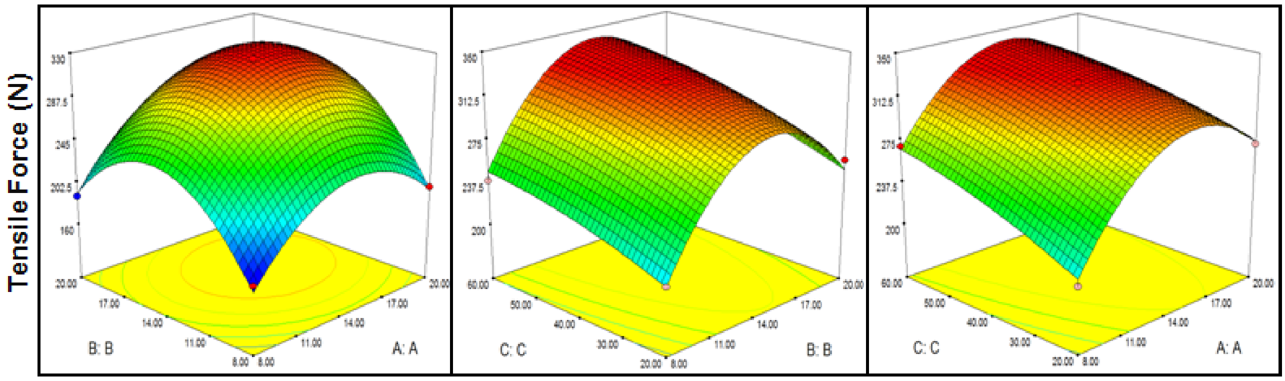

Fig.8 The effects of process parameters on the tensile forces

Process parameters such as heating time, cooling time, and air flow rate have significant and complex effects on objective function. These process parameters also have contradictory effects on responses. To solve the optimization problem, the evolution algorithm, namely Multi-Island GA is adopted. Specific parameters were population size, number of generations, crossover probability, crossover distribution index, and mutation distribution index, with values of 10, 20, 0.9, 20, and 100, respectively. Figure 9 describes the history of the NSGA II-based optimization process.

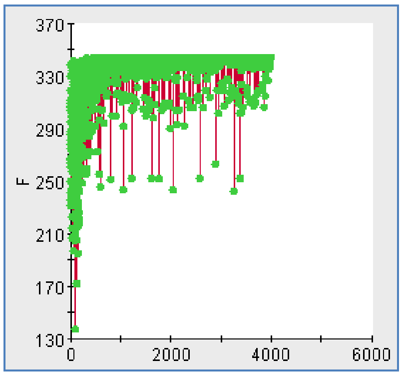

Fig.9 History of GA solving process

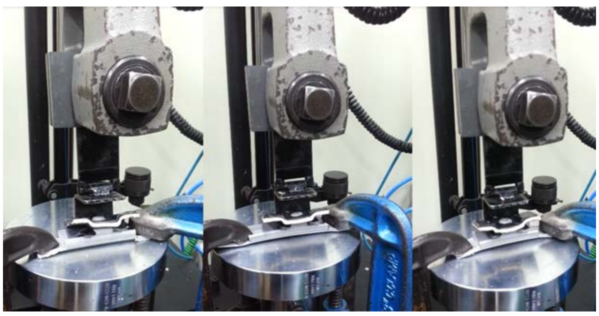

Fig.10 Tensile testing at the company

The optimal parameters, including heating time, cooling time, and air flow rat are 14, 14 second, 60, respectively. To validate the proposed method, the physical staking process was conducted in HANIL EHWA-Door Trim Manufacturer in South Korea. The error between simulation and experimental results is lower 10% that indicates the effectiveness of the proposed method.

Table 3 Optimization values

Design variables			Tensile Force (N)	
A (s)	B (s)	C (ft^3/h)	Simulation	Experiment
14	14	60	348.81	362.8

Conclusion

This paper presents a new approach to simulate and optimize infrared staking process. The FE model considering the interaction between sub-process has been developed using DEFORM-3D in order to investigate the effects of process parameters on the mechanical behavior. The maximizing tensile force can be achieved at optimal parameters in 14, 14 second, and 60 (ft^3/h) of heating time, cooling time, and air flow rate, respectively. The optimal results also indicated that heating time is more contribution to tensile strength compared to the others. The proposed method can be used as the effective approach to simulate and optimize the process chains. The effects of forming tool geometry on the mechanical behavior of the joint will be analyzed in future work.

Acknowledgement

This work was supported by the Research Fund of the University of Ulsan (2015) and Brain Korea 21 plus program.

References

Information http://www.extolinc.com/infrastake

Fluhrer, J., DEFORMTM-3D Version 5.0 User's Manual, Scientific Forming Technologies Corporation, 2005

C.F. Jeff, R. C. Z., Y. Lan (2000), Experiment Design & Analyses and Parameters Optimization, Wiley.

M. Oudjene, L. Ben-Ayed, A. Delamézière, J.-L. Batoz (2009) Shape optimization of clinching tools using the response surface methodology with Moving Least-Square approximation, *Journal of Materials Processing Technology* **209**, 289-296

F. Lambiase, A. Di Ilio (2013) Optimization of the clinching tools by means of integrated FE modeling and artificial intelligence techniques, *Procedia CIRP* **12** 163-168

YUANXIN ZHOU, P. K. MALLICK (2002), Effects of Temperature and Strain Rate on the Tensile Behavior of Unfilled and Talc-Filled Polypropylene. Part I: Experiments, *Polymer Engineering & Science* **42**, 2461-2470

Matweb, Material Property Data.

Carlaw, H. and Jaeger, J., (1959) Conduction of heat in solids, *Oxford at the Clarendon Press* **2**, 17-25.